

Electron energy loss spectroscopy in ACrO_3 (A = Ca, Sr and Pb) perovskites

This article has been downloaded from IOPscience. Please scroll down to see the full text article.

2008 J. Phys.: Condens. Matter 20 505207

(<http://iopscience.iop.org/0953-8984/20/50/505207>)

View [the table of contents for this issue](#), or go to the [journal homepage](#) for more

Download details:

IP Address: 129.252.86.83

The article was downloaded on 29/05/2010 at 16:49

Please note that [terms and conditions apply](#).

Electron energy loss spectroscopy in ACrO_3 ($A = \text{Ca, Sr and Pb}$) perovskites

Ángel M Arévalo-López, Elizabeth Castillo-Martínez and Miguel Á Alario-Franco¹

Departamento de Química Inorgánica I, Facultad CC. Químicas, UCM, 28040 Madrid, Spain

E-mail: maaf@quim.ucm.es

Received 8 September 2008, in final form 15 October 2008

Published 7 November 2008

Online at stacks.iop.org/JPhysCM/20/505207

Abstract

We present the experimental ELNES spectra of the Cr- $L_{2,3}$ and O-K edges in three high pressure synthesized perovskites, ACrO_3 ($A = \text{Ca, Sr and Pb}$). A comparison of the experimental spectra against the theoretical calculations shows the influence of the A cation in the features of the spectrum. The Cr- $L_{2,3}$ multiplet structure of these perovskites shows similar integrated intensity ratio ($\int I_{L_3} / \int I_{L_2}$) between them and with the CrO_2 , implying that all of them are indeed composed by Cr^{4+} . But the O-K pre-edge observed in CrO_2 , typical of its d^3L character (L-ligand hole), is not present in these perovskites. The effect of the A cation manifests itself in the O-K edge. The different features in the peak edges are caused by the change in the interaction between oxygen and the A cation from being via p orbitals (with Pb) to being via d orbitals (with Ca, Sr). The experimental spectra of the samples are reproduced well by the presented DFT calculations.

(Some figures in this article are in colour only in the electronic version)

1. Introduction

The study of the perovskite-type transition-metal oxides with nd electrons has attracted much interest in recent years due to their wide range of interesting properties and to the possibility of varying these. The high pressure chromium perovskites $\text{ACr}^{4+}\text{O}_3$ ($A = \text{Sr, Ca and Pb}$), which present Cr^{4+} in octahedral coordinations as in the half-metal ferromagnet, CrO_2 , have rarely been studied because of their synthetic difficulties: they need high pressure to be formed and can hardly be obtained in a pure form. They were first synthesized in the late 1960s, and recently, there has been a renewed interest in them. SrCrO_3 is an ideal cubic perovskite ($Pm\bar{3}m$), and there is still no explanation for the differences encountered in both the electronic (metal–semiconductor) and magnetic (Pauli paramagnetic–Curie Weiss behavior) properties reported by different authors [1–5]. CaCrO_3 is an orthorhombic perovskite ($Pbnm$) with a transition from a paramagnetic to a canted antiferromagnetic state below 90 K [6–8]. It was originally found that polycrystalline samples were semiconducting, whereas single crystals, eventually with a different stoichiometry, were metallic. Recent reports also

show the same controversy [3], but a combined study on both single crystals and a polycrystalline sample give evidence of the metallic nature of CaCrO_3 by optical conductivity and reflectivity measurements [9].

PbCrO_3 was reported to be antiferromagnetic and semiconducting [10–12]. A recent study has shown that it presents a very complex microstructure which by powder x-ray diffraction is averaged to a cubic one [13]. The approximate stoichiometry is $\text{Pb}_{0.9}\text{CrO}_{2.9}$, as deduced from the cationic analysis from electron microscopy. Nevertheless some oxygen deficiency, concomitant with an intermediate chromium valence cannot be ruled out.

Electron microscopy techniques have allowed us to characterize the microstructure of individual crystals well [8, 13]. Coupled to the transmission electron microscope (TEM), electron energy loss spectroscopy (EELS) can also be used to analyze single crystals. This technique has been widely used to determine the valence state and coordination environment of the transition-metal cation in titanates, manganates and ferrites [14–17]. However in the Cr compounds studied so far, it has been rather difficult to unambiguously determine the valence and/or coordination number. Daulton and Little proved this intrinsic difficulty in deducing the valence state in

¹ Author to whom any correspondence should be addressed.

Table 1. Energy positions of the O-K and Cr-L edges in the EELS spectra labeled in figure 1(a), Δ represents the difference between adjacent peaks: $\Delta_1 = b-a$, $\Delta_2 = c-b$, $\Delta_3 = d-c$ and $\Delta_4 = e-d$.

	O-K (eV)		O-K (eV)		O-K (eV)		Cr-L ₂ (eV)		Cr-L ₃ (eV)		$\int I_{L_3} / \int I_{L_2}$
	a	Δ_1	b	Δ_2	c	Δ_3	d	Δ_4	e		
CaCrO ₃	529.2	5.4	534.6	6.6	541.2	35.1	576.3	8.7	585	1.46	
SrCrO ₃	528.1	6.6	534.7	6.4	541.1	35.2	576.3	8.4	584.7	1.39	
PbCrO ₃	529.1	—	—	—	539.5	37	576.3	8.4	584.9	1.48	

Cr compounds (although the range of possible valences can be constrained) but they had used only one Cr⁴⁺ compound (CrO₂) to establish the correlation between peak positions/ratio versus oxidation state [18]. In addition, Suzuki and Tomita had stated the importance of the O-K edge in Cr(III) and Cr(IV) compounds; they demonstrated that while no substantial differences in the Cr-L_{2,3} edges between CrO₂ and Cr₂O₃ could be observed, differences between the two compounds are seen in the threshold of the O-K spectra [19]. In this study a d³L configuration was established by the appearance of an extra peak at low energies in the XPS and EEL spectra of CrO₂. This Cr³⁺-O²⁻ hole, or self-doping, is considered to be responsible of the half-metallic behavior found in CrO₂ [20].

Previous theoretical studies based on linear muffin tin orbital (LMTO) calculations predicted a metallic behavior for both SrCrO₃ and PbCrO₃ [21] but the introduction of the Hubbard interaction parameter (U) in PbCrO₃ produces a change in the predicted properties from metallic to semiconducting as has been experimentally determined [12]. The introduction of the Hubbard parameter only causes a shift in the energy levels, consequently creating a band gap, but the general trend of the DOS remains without alteration. This has also been observed by other authors [22–24]. On the same lines, Komarek *et al* performed LSDA calculations on CaCrO₃ with and without the inclusion of the Hubbard parameter. They concluded that the correct ground state is given by the calculations made without this parameter, since these reproduced the electronic properties [9].

We present here an experimental EELS study performed on individual single crystals of the ACr⁴⁺O₃ perovskites (A = Ca, Sr and Pb) selected in the electron microscope; this, coupled to theoretical calculations, have allowed us to make an identification of the interactions that produce these spectra as well as to establish the reasons for their differences. Our calculations have been performed without considering the Hubbard parameter since it does not greatly affect the description of the empty states and no real distinction can be made between these two descriptions of the EEL spectrum [25]. The absence of self-doping in any of these Cr⁴⁺ compounds, as compared to CrO₂, is established by the lack of the corresponding spectral line. Although in these compounds Cr has the same electronic configuration and coordination environment as in CrO₂, they do not present either the ferromagnetic or the negative charge transfer gap behavior.

2. Experimental details

The synthesis, structural features and physical properties of the samples used in this study, are described in previous

publications [8, 4, 13, 26]. For the acquisition of the EEL spectra we used an ENFINA EELS system placed on a JEOL JEM 3000FEG microscope, operating at 300 keV in the diffraction mode with a collection semiangle of 8.9 mrad and a dispersion of 0.2 eV/channel. To ensure that the EELS measurements are not dependent on sample orientation, all the spectra were collected in diffraction mode far away from zone axes. Under these conditions, the product of the momentum transfer and the extent of the core electron wavefunction is sufficiently smaller than unity and the core-level energy loss spectra are well described by the dipole transition [27]. The stability of the samples under the electron beam has been tested with selected area electron diffraction (SAED) prior to and after the EELS acquisition to ensure no extra maxima have appeared as a consequence of any beam damage that may cause loss of oxygen and a change in the valences. The background has been subtracted with an inverse power law fitting, and plural scattering contributions were removed using the Fourier-ratio deconvolution technique [28]. For a proper comparison, we have corrected the energy scale by fixing the Cr-L₃ edge to the value obtained by XPS for Cr⁴⁺ in CrO₂, namely 576.3 eV [29] (table 1).

The EEL spectra and the density of states (DOS) have been calculated using the WIEN2K package [30, 31], which is an implementation of the hybrid full potential linear augmented plane wave plus local orbitals (LAPW + lo) method within the density-functional theory (DFT). We used the Perdew–Burke–Ernzerhof generalized gradient approximation (GGA) for the exchange correlation potentials [32]. Relativistic effects were taken into account within the scalar-relativistic approximation. The k -point sampling in the Brillouin zone was conducted with a $10 \times 10 \times 10$ mesh. The self-consistent calculations were carried out with a total energy convergence tolerance of less than 0.1 mRyd. The difference in energy and intensity ratio of the Cr-L_{2,3} edge were initially introduced into the calculations. The measurement of the experimental L₃/L₂ ratio of integrated peak intensities has been made over a 5 eV integration width around the maxima of each peak after a background subtraction following Pearson’s method [33]. The theoretical electron loss near edge structure (ELNES) spectra used for comparison were obtained with the non-polarized approximation since, at the temperature at which the spectra were recorded, room temperature, the samples were in the paramagnetic state. The broadening used for the calculation of the spectra was the taken from value observed at full width at half maximum (FWHM) of the zero loss peak (ZLP) of the experimental spectra (1.0 eV).

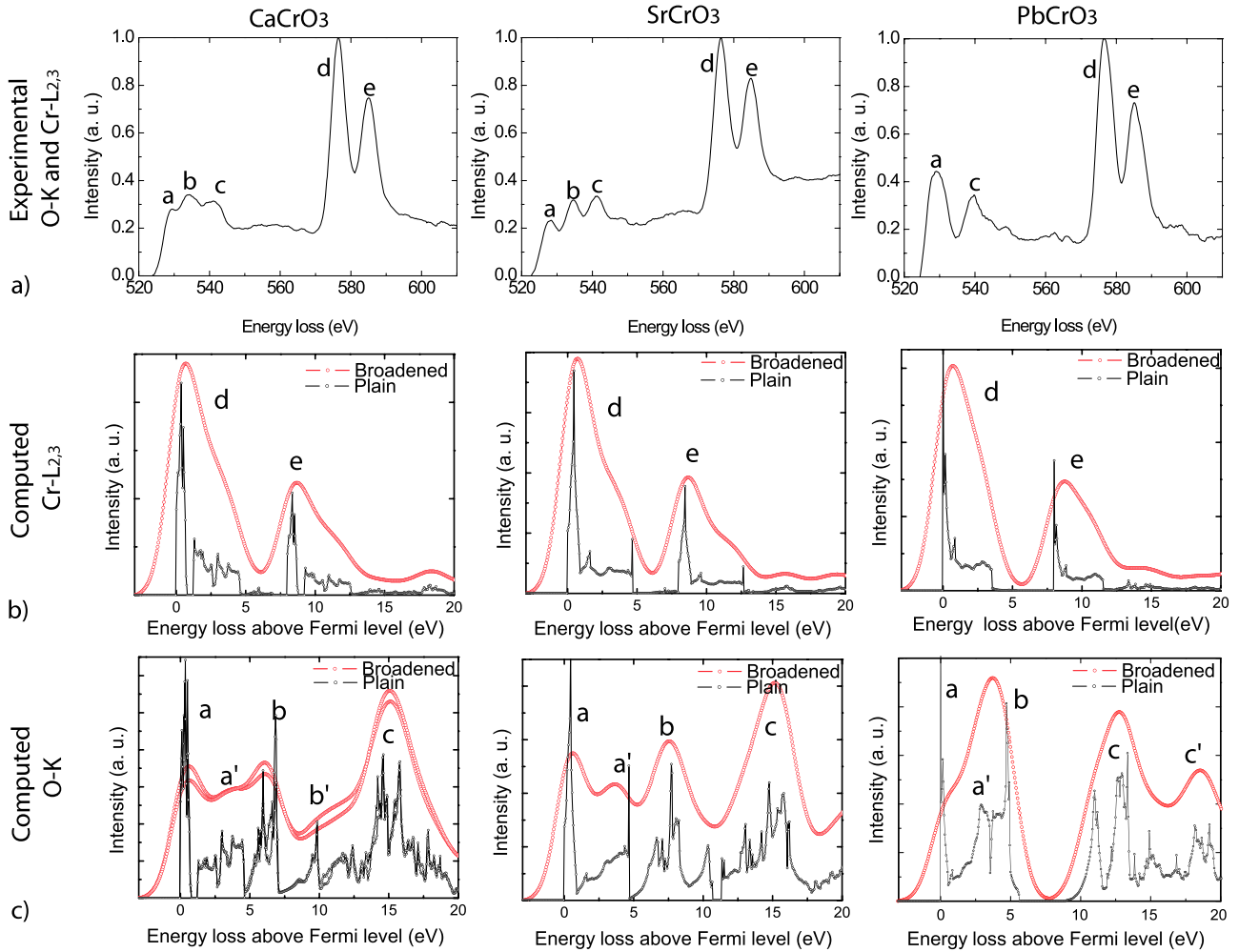


Figure 1. Experimental (top) and calculated EELS spectra for the O-K (middle) and Cr-L_{2,3} (bottom) for the ACr⁴⁺O₃ (A = Ca, Sr and Pb) perovskites. With and without considering broadening. For CaCrO₃ the two different oxygen atoms O₁ and O₂ appear superposed [8]. The splitting of the Cr-L_{2,3} edges as well as their intensity ratio are introduced *a priori* into the calculations.

3. Results

The O-K and Cr-L_{2,3} absorption edges of the experimental energy loss spectra for the Cr⁴⁺ high pressure perovskites ACrO₃ (A = Ca, Sr, and Pb) are shown in figure 1(a). The computed Cr and O EEL peaks of the analyzed oxides are also represented in figures 1(b) and (c), respectively.

The maxima of the experimental and calculated spectra are labeled with a, b, c, d and e respectively. Their experimental energy positions are given in table 1 and the calculated values appear in table 2. The differences between adjacent maxima, Δ , are also listed. Δ_4 and the ratio of intensities, which were initially introduced for the calculation, are, therefore, not included in table 2.

The Cr-L_{2,3} edge roughly separates into two regions due to spin-orbit split of 2p orbitals (peaks d and e). It is clear that the spectra in this last region are practically the same in these ACrO₃ compounds, however, a small dispersion is found for the L₃/L₂ integrated intensity ratio in the experimental spectra (1.39–1.48, table 1). Nonetheless, these values are in agreement with the one reported for the CrO₂ (1.48) calculated by the same method [18].

Concerning the O-K edge, the spectrum of PbCrO₃ only shows two peaks, while for SrCrO₃ and CaCrO₃ there are three well resolved main peaks. Figures 2(a) and (b) show the calculated ELNES spectra for the Cr-L₃ and the O-K edges for the three perovskites along with the DOS that gives rise to their trends respectively, while, in figure 2(c) the total DOS for each atom is presented; here it is possible to establish the interactions between the ions.

4. Discussion

From the appearance of the experimental EELS (figure 1(a)), the positions of the maxima and the L₃/L₂ integrated intensity ratio (table 1), one can see that there are no significant differences in the Cr edge between these compounds. Furthermore, the values of the $\int I_{L_3} / \int I_{L_2}$ ratio in the three perovskites are slightly smaller or equal to the value reported for CrO₂ (1.48 or 1.55, depending on the method), while for Cr³⁺ oxides it is 1.68, 1.62 or 1.60 for Cr₂O₃, NdCrO₃ or LaCrO₃, respectively [18]. Thus, this indicates a Cr⁴⁺ or higher valence state, which would be very unusual [26].

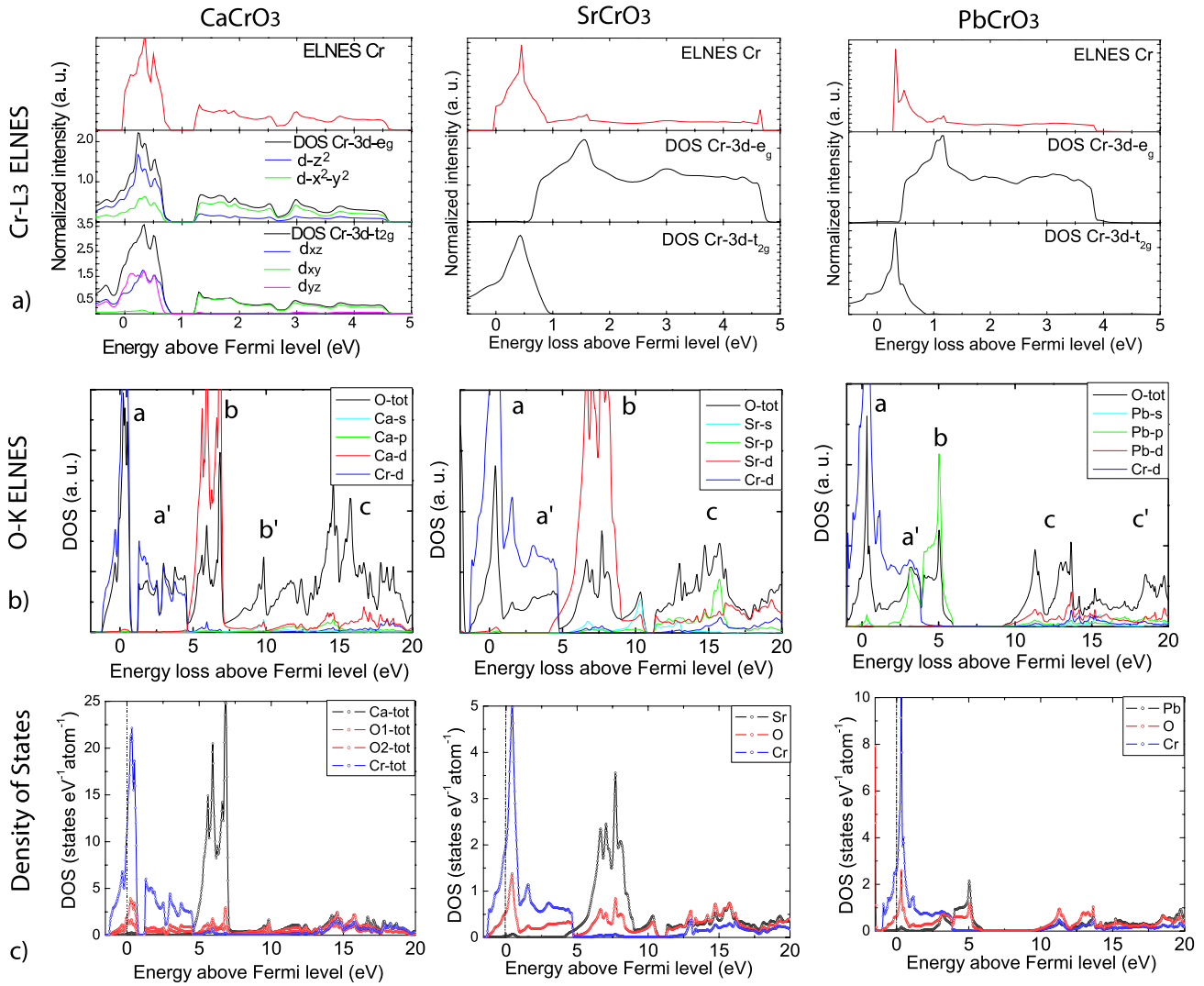


Figure 2. Calculated ELNES spectra for the Cr-L₃ and O-K edges (top) without broadening, and total and partial DOS for A, Cr and O ions (A = Ca, Sr and Pb). For the CaCrO₃ DOS graph, the two oxygens are superposed.

Table 2. Energy positions of the O-K and Cr-L_{2,3} edges in the calculated EELS spectra labeled in figures 1(b) and (c), Δ represents the difference between adjacent peaks: $\Delta_1 = b - a$, $\Delta_2 = c - b$.

Perovskite/peak	O-K (eV)			O-K (eV)			O-K (eV)		Cr-L ₂ (eV)	Cr-L ₃ (eV)
	a	a'	Δ_1	b	b'	Δ_2	c	c'		
CaCrO ₃	0.35	3.45	5.7	6.05	10.0	9.35	15.05	—	0.65	8.65
SrCrO ₃	0.55	3.65	3.85	7.5	—	7.55	15.05	—	0.65	8.65
PbCrO ₃	0.0	2.9	4.7	4.7	—	8.25	12.95	18.25	1.15	9.15

Cr-L_{2,3} edges (d and e) arises from excitations of electrons in 2p \rightarrow 3d orbitals. Figure 2(a) shows the calculated Cr-L₃ edge. In the case of SrCrO₃ and PbCrO₃ the edge mainly comes from transitions to degenerate t_{2g} orbitals. However, in the case of CaCrO₃ (*Pbnm*), where the orthorhombic distortion removes the t_{2g} and e_g orbital degeneracy, the energies of these orbitals are closer and a mixed composition of the Cr-L_{2,3} peak can be observed, due to transitions to both ‘t_{2g}’ and ‘e_g’ orbitals.

The features of the O-K edge for SrCrO₃ and CaCrO₃ are quite similar (figure 1(c)). The first two calculated peaks

(a and a’) come from the hybridization between O and Cr (figure 2(b)). The next one (b) arises from the hybridization between Sr or Ca with O. In the case of CaCrO₃, there is also another small peak (b’). This maximum is also caused by interactions between Ca and O. The last one (labeled c), is due to interactions of both cations, Sr(Ca) and Cr, with oxygen. On the other hand, the O-K edge for PbCrO₃, shows only two broad peaks (a and c). However the DFT calculations show that each peak is formed by two, a–b and c–c’ respectively. The first one, a, comes from interactions between the Cr and the O; these interactions are also responsible for the Cr-L edges. The

second one, b, arises from interactions between Pb and O. The overlap of these two peaks gives an experimental a peak more intense than those of the Ca and Sr perovskites. The c and c' peaks arise from higher level interactions from both Pb and Cr with O, as in CaCrO₃ and SrCrO₃.

The main differences between Sr(Ca)CrO₃ and PbCrO₃ are on the oxygen K edge. We have observed that Cr–O and Pb–O, a and b peaks, overlap because the Pb–O interactions take place through Pb-p orbitals and not through d orbitals as in Sr or Ca, therefore the Pb–O peak (b) is shifted to lower energy values, 4.7 eV versus 6.05 or 7.5 eV in Ca or Sr respectively, see table 2.

The PbCrO₃ a' peak arises from interactions of both Cr and Pb with O. In addition, since this material presents a complex modulation, there are inequivalent oxygen sites, but, the complexity of this structure prevents the incorporation of these sites into the calculations and a weighted average projected DOS (and consequently, the ELNES) is forced since the start of the calculations considers just the average cubic structure. Moreover, since PbCrO₃ is off-stoichiometric, it is very likely that a small quantity of Cr³⁺ should be present, or at least some of the Cr⁴⁺ atoms would present a different oxygen environment. All of this affects the EELS data, and the superposition of both spectra (the one arising from Cr⁴⁺ and the one from Cr³⁺ or with a different oxygen environment) and/or the inequivalent oxygen sites give this broadening of the spectrum.

From figure 2(c) one can see that the interaction between the O and the A cation diminishes as Z increases, like the ionic potential (Z/r). Despite the differences between the spectra of these three perovskites they also have common features that are distinct from those of CrO₂. These are: the absence of an absorption line at lower energy values and lower $\int I_{L_3} / \int I_{L_2}$ ratio with respect to all the Cr³⁺ compounds listed by Daulton and Little [18] as well as those Cr³⁺ perovskites that we have experimentally studied. This corresponds to a higher oxidation state and indicates the absence of self-doping in Cr⁴⁺ perovskites against CrO₂.

5. Conclusions

We present experimental EEL spectra of three Cr⁴⁺-based high pressure perovskites. Although the main differences between the spectra are not observed in the L_{2,3} edges as happens in CrO₂ and Cr₂O₃ [19] a $\int I_{L_3} / \int I_{L_2}$ value in agreement with Cr⁴⁺ is obtained. Besides the Cr-L_{2,3} edges, we have also considered the O-K edge in order to make a determination of the different interactions in these Cr-based compounds. In the case of PbCrO₃, we observe two maxima in that region and three in those of SrCrO₃ and CaCrO₃. By using a simple comparison between the experimental spectra, the calculated DOS and ELNES spectra, we have been able to identify the origin of the differences in the O-K edges. Moreover, neither the different symmetry nor the octahedral distortion in CaCrO₃ seriously affects the EEL spectrum, it is very similar to the one for SrCrO₃, however, the complex microstructure of PbCrO₃ does modify it. On the other hand, even though in these perovskites, Cr has the same electronic configuration and the

same oxygen environment as in CrO₂, the EEL spectra indicate that they do not present the self-doping behavior characterized by the O-K pre-edge found for CrO₂ [19].

Acknowledgments

We thank Nebil Ayape Katcho and Dr. David Avila Brande for valuable and fruitful discussions. The authors also want to thank CONACYT México and UCM for their financial support. CICYT through projects MAT2004-01641 and MAT2007-64006, Comunidad Autónoma de Madrid, MATERYENER program, PRICYT S-0505/PPQ-0093 (2006) and the Areces Foundation through its program 'Ayudas 2004' also gave financial support. We also thank the x-ray CAI and electron microscopy center of UCM. Samples were obtained from LABCOAP (<http://www.ucm.es/info/labcoap/index.htm>) with the help of Dr Jose Manuel Gallardo Amores.

References

- [1] Chamberland B L 1967 *Solid State Commun.* **5** 663
- [2] Williams A J, Gillies A, Attfield J P, Heymann G, Huppertz H, Martinez-Lopez M J and Alonso J 2006 *Phys. Rev. B* **73** 104409
- [3] Long Y W, Yang L X, Zhou J S, Jin C Q and Goodenough J B 2006 *Phys. Rev. Lett.* **96** 046408
- [4] Castillo-Martinez E and Alario-Franco M A 2007 *Solid State Sci.* **9** 564
- [5] Ortega-San-Martin L, Williams A J, Rodgers J, Attfield J P, Heymann G and Huppertz H 2007 *Phys. Rev. Lett.* **99** 255701
- [6] Kafalas J A, Goodenough J B and Longo J M 1968 *Mater. Res. Bull.* **3** 471
- [7] Weiher J F, Chamberland B L and Gillson J L 1971 *J. Solid State Chem.* **3** 529
- [8] Castillo-Martinez E, Duran A and Alario-Franco M A 2008 *J. Solid State Chem.* **181** 895
- [9] Komarek A C *et al* 2008 arXiv:0804.1071
- [10] Roth W L and DeVries R C 1967 *J. Appl. Phys.* **38** 951
- [11] DeVries R C and Roth W L 1968 *J. Am. Ceram. Soc.* **51** 72
- [12] Chamberland B L and Moeller C W 1972 *J. Solid State Chem.* **5** 39
- [13] Arevalo-Lopez A M and Alario-Franco M A 2007 *J. Solid State Chem.* **180** 3271
- [14] Potapov P L, Jorissen K, Schryvers D and Lamoen D 2004 *Phys. Rev. B* **70** 045106
- [15] Kurata H and Colliex Ch 1993 *Phys. Rev. B* **48** 2102
- [16] Riedl T, Gemming T and Wetzig K 2006 *Ultramicroscopy* **106** 284
- [17] Stoyanov E, Langenhorst F and Steidle-Neumann G 2007 *Am. Mineral.* **92** 577
- [18] Daulton T L and Little B J 2006 *Ultramicroscopy* **106** 561
- [19] Suzuki S and Tomita M 1997 *Japan. J. Appl. Phys.* **36** 4341
- [20] Korotin M A, Anisimov V I, Khomskii D I and Sawatzky G A 1998 *Phys. Rev. Lett.* **80** 4305
- [21] Jaya S M, Jagadish R, Rao R S and Asokamani R 1992 *Mod. Phys. Lett. B* **6** 103
- [22] Cao Y L, Yu W H, Wang L L, Cai M Q, Yang G W and Wang Y G 2007 *Appl. Phys. Lett.* **90** 242911
- [23] Hatt A J and Spaldin N A 2007 *Appl. Phys. Lett.* **90** 242916
- [24] Mazin I I, Khomskii D I, Lengsdorf R, Alonso J A, Marshall W G, Ibberson R M, Podlesnyak A, Martinez-Lopez M J and Abd-Elmeguid M M 2007 *Phys. Rev. Lett.* **98** 176406

- [25] de Groot F M F 1994 *J. Electron Spectrosc. Relat. Phenom.* **67** 529
- [26] Castillo-Martinez E, Arevalo-Lopez A M, Ruiz-Bustos R and Alario-Franco M A 2007 *Inorg. Chem.* **47** 8526
- [27] Muller D A, Singh D J and Silcox J 1998 *Phys. Rev. B* **57** 8181
- [28] Egerton R F 1996 *Electron Energy-Loss Spectroscopy in the Electron Microscope* (New York: Plenum)
- [29] Ikemoto I, Ishii K, Kinoshita S, Kuroda H, Alario-Franco M A and Thomas J M 1976 *J. Solid State Chem.* **17** 425
- [30] Blaha P, Schwarz K, Sorantin P and Trickey S B 1990 *Comput. Phys. Commun.* **59** 399
- [31] Madsen G K H, Kvasnicka D, Blaha P, Schwarz K and Luitz J 2001 *Computer code WIEN2k* Technische Universität Wien, Austria
- [32] Perdew J P, Burke K and Ernzerhof M 1996 *Phys. Rev. Lett.* **77** 3865
- [33] Ahn C C, Pearson D H and Fultz B 1993 *Phys. Rev. B* **47** 8471